

See discussions, stats, and author profiles for this publication at: <https://www.researchgate.net/publication/6558947>

Interaction between Block Copolymer Micelles and Azobenzene-Containing Surfactants: From Coassembly in Water to Layer-by-Layer Assembly at the Interface

ARTICLE in LANGMUIR · MARCH 2007

Impact Factor: 4.46 · DOI: 10.1021/la0632068 · Source: PubMed

CITATIONS

40

READS

42

7 AUTHORS, INCLUDING:



Ning Ma

University of Science and Technology Beijing

30 PUBLICATIONS 1,496 CITATIONS

SEE PROFILE



Zhiqiang Wang

Wuhan University

179 PUBLICATIONS 8,302 CITATIONS

SEE PROFILE

Interaction between Block Copolymer Micelles and Azobenzene-Containing Surfactants: From Coassembly in Water to Layer-by-Layer Assembly at the Interface

Ning Ma, Yapei Wang, Baoyu Wang, Zhiqiang Wang, and Xi Zhang*

Key Lab of Organic Optoelectronics and Molecular Engineering, Department of Chemistry, Tsinghua University, Beijing 100084, and Key Lab for Supramolecular Structure and Materials, College of Chemistry, Jilin University, Changchun 130012, People's Republic of China

Guang Wang and Yue Zhao

Département de chimie, Université de Sherbrooke, Sherbrooke, Québec, Canada J1K 2R1

Received November 2, 2006. In Final Form: December 8, 2006

In this paper, we describe the use of block copolymer micelles to incorporate Azo-AOT, an azobenzene-containing amphiphile having a structure suitable for reverse micelle formation and the fabrication of polyelectrolyte/micelle multilayer films. Interestingly, it is found that the PS₂₁–PAA₁₅₇ micelles can incorporate more Azo-AOT molecules than the PS₁₁₅–PAA₁₅ micelles, which is different from the case of incorporation of noncharged hydrophobic molecules. Moreover, Azo-AOT incorporated into the PS₂₁–PAA₁₅₇ micelles undergoes a faster photoisomerization than in the PS₁₁₅–PAA₁₅ micelles, which seems to be related to different aggregation states of Azo-AOT in the two micelles. From the data of UV–vis spectra, we can infer that Azo-AOT adopts a reverse micelle-like aggregation state in the PS₁₁₅–PAA₁₅ micelles and disperses in the interface between the core and corona of PS₂₁–PAA₁₅₇ micelles. These polyelectrolyte/micelle films incorporating functional amphiphiles have great potential in the field of functional thin films.

Introduction

Layer-by-layer (LbL) assembly, which was first introduced in the 1960s and rediscovered in the 1990s, has proven to be a versatile method for fabricating nanoscaled composites and assemblies.¹ This method has exhibited several advantages including simplicity, convenience, and easy control of the properties of the films. For these reasons, numerous functional materials have become good candidates for the LbL fabrication, including oligocharged dyes,² inorganic compounds,³ photoreactive species,⁴ thermoresponsive materials,⁵ biomacromolecules⁶ and so forth, which have endowed the multilayer films with various compositions and functions. Moreover, to make it possible to assemble some water-insoluble polymers by this approach, many intermolecular interactions have been developed as driving forces for the fabrication of the LbL films, such as hydrogen

bond,⁷ coordination bond,⁸ charge-transfer interaction,⁹ and chemical reaction.¹⁰

Azobenzene derivatives are an important family of chromophores which can be used as optical switches for photoactive systems.¹¹ In the past few years, there have been numerous reports about LbL assembly of azobenzene-containing polymers and amphiphiles with polyelectrolytes for fabricating multilayer films with photoresponsive properties or ordered layered structures,¹² but some water-insoluble azobenzene derivatives are still difficult to assemble into the LbL films. Recently, we introduced a method which combines precursor assembly and LbL deposition for assembling some noncharged organic species or singly charged functional molecules which cannot be assembled by the conventional LbL method.^{13,14} By this method, the block copolymer micelles were used to incorporate azobenzene and

* To whom correspondence should be addressed at Tsinghua University. Fax: 0086-10-62771149. E-mail: xi@mail.tsinghua.edu.cn.

(1) (a) Iler, R. K. *J. Colloid Interface Sci.* **1966**, *21*, 569. (b) Decher, G.; Hong, J.-D. *Makromol. Chem., Macromol. Symp.* **1991**, *46*, 321. (c) Decher, G. *Science* **1997**, *277*, 1232. (d) Zhang, X.; Shen, J. C. *Adv. Mater.* **1999**, *11*, 1139. (e) Zhang, X.; Chen, H.; Zhang, H. Y. *Chem. Commun.* **2006**, in press.

(2) (a) Zhang, X.; Gao, M. L.; Kong, X. X.; Sun, Y. P.; Shen, J. C. *J. Chem. Soc., Chem. Commun.* **1994**, 1055. (b) Saremi, F.; Tiek, B. *Adv. Mater.* **1998**, *10*, 388. (c) Tedeschi, C.; Caruso, F.; Möhwald, H.; Kirstein, S. *J. Am. Chem. Soc.* **2000**, *122*, 5841. (d) Advincula, R. C.; Fells, E.; Park, M. K. *Chem. Mater.* **2001**, *13*, 2870.

(3) (a) Kleinfeld, E. R.; Ferguson, G. S. *Science* **1994**, *265*, 370. (b) Caruso, R. A.; Susha, A.; Caruso, F. *Chem. Mater.* **2001**, *13*, 400.

(4) Sun, J. Q.; Wu, T.; Sun, Y. P.; Wang, Z. Q.; Zhang, X.; Shen, J. C.; Cao, W. X. *Chem. Commun.* **1998**, 1853.

(5) (a) Quinn, J. F.; Caruso, F. *Langmuir* **2004**, *20*, 20. (b) Quinn, J. F.; Caruso, F. *Macromolecules* **2005**, *38*, 3414.

(6) (a) Kong, W.; Zhang, X.; Gao, M. L.; Zhou, H.; Li, W.; Shen, J. C. *Macromol. Rapid Commun.* **1994**, *15*, 405. (b) Lvov, Y.; Lu, Z.; Schenkman, J. B.; Zu, X.; Rusling, J. F. *J. Am. Chem. Soc.* **1998**, *120*, 4073. (c) Picart, C.; Lavalle, Ph.; Hubert, P.; Cuisinier, F. J. G.; Decher, G.; Schaaf, P.; Voegel, J.-C. *Langmuir* **2001**, *17*, 7414. (d) Serizawa, T.; Yamaguchi, M.; Akashi, M. *Macromolecules* **2002**, *35*, 8656. (e) Yu, A.; Liang, Z.; Caruso, F. *Chem. Mater.* **2005**, *17*, 171.

(7) (a) Wang, L. Y.; Wang, Z. Q.; Zhang, X.; Shen, J. C.; Chi, L. F.; Fuchs, H. *Macromol. Rapid Commun.* **1997**, *18*, 509. (b) Stockton, W. B.; Rubner, M. F. *Macromolecules* **1997**, *30*, 2717.

(8) (a) Xiong, H. M.; Cheng, M. H.; Zhou, Z.; Zhang, X.; Shen, J. C. *Adv. Mater.* **1998**, *10*, 529. (b) Kohli, P.; Blanchard, G. J. *Langmuir* **2000**, *16*, 8518.

(9) Shimazaki, Y.; Mitsuishi, M.; Ito, S.; Yamamoto, M. *Langmuir* **1997**, *13*, 1385.

(10) (a) Zhang, F.; Jia, Z.; Srinivasan, M. P. *Langmuir* **2005**, *21*, 3389. (b) Such, G. K.; Quinn, J. F.; Quinn, A.; Tjipto, E.; Caruso, F. *J. Am. Chem. Soc.* **2006**, *128*, 9318.

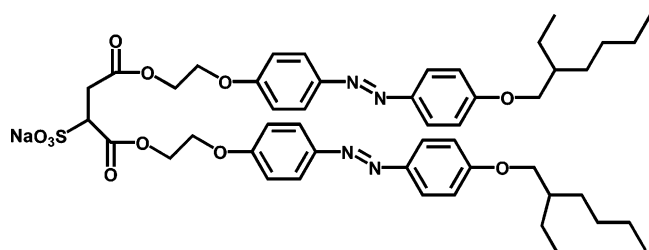
(11) Rau, H. Photoisomerization of Azobenzenes. In *Photochemistry and Photophysics*; Rabek, J. F., Ed.; CRC Press: Boca Raton, FL, 1990; Vol. 2, p 119.

(12) (a) Dante, S.; Advincula, R.; Frank, C. W.; Stroeve, P. *Langmuir* **1999**, *15*, 193. (b) Hong, J.-D.; Park, E.-D.; Park, A.-L. *Langmuir* **1999**, *15*, 6515. (c) Lee, S.-H.; Balasubramanian, S.; Kim, D. Y.; Viswanathan, N. K.; Bian, S.; Kumar, J.; Tripathy, S. K. *Macromolecules* **2000**, *33*, 6534. (d) Arys, X.; Fischer, P.; Jonas, A.; Koetse, M.; Laschewsky, A.; Legras, R.; Wischerhoff, E. *J. Am. Chem. Soc.* **2003**, *125*, 1859.

(13) (a) Ma, N.; Zhang, H. Y.; Song, B.; Wang, Z. Q.; Zhang, X. *Chem. Mater.* **2005**, *17*, 5065. (b) Ma, N.; Wang, Y. P.; Wang, Z. Q.; Zhang, X. *Langmuir* **2006**, *22*, 3906.

(14) Chen, H.; Zeng, G. H.; Wang, Z. Q.; Zhang, X.; Peng, M.-L.; Wu, L.-Z.; Tung, C.-H. *Chem. Mater.* **2005**, *17*, 6679.

Scheme 1. Chemical Structure of Azo-AOT



then the azobenzene-incorporated micelles were employed to fabricate the multilayer films by alternating deposition with polyelectrolytes. It was demonstrated that the photoisomerization properties of photoswitching molecules could be improved in their solid films within the microenvironments provided by the block copolymer micelles. Until now, the molecules incorporated into block copolymer micelles have all been noncharged hydrophobic species,^{13,15} and to our best knowledge, there are no reports on the use of block copolymer micelles to incorporate or to coassemble with azobenzene-containing amphiphiles whose structures promote the formation of reverse micelles. In this study, we attempted to use the block copolymer micelles to incorporate such an amphiphile, Azo-AOT, and assembled them into the LbL films. Moreover, we wondered whether different core–shell micellar structures could influence the photoisomerization of Azo-AOT either in the bulk micellar solutions or in the multilayered polyelectrolyte/micelle films.

Experimental Section

Materials. Three samples of the amphiphilic diblock copolymer of poly(styrene-*b*-acrylic acid) (M_n , PS(12000)–PAA(1100), $M_w/M_n = 1.10$; M_n , PS(2200)–PAA(11300), $M_w/M_n = 1.10$) and poly(styrene-*b*-methacrylic acid) (M_n , PS(6500)–PMAA(21600), $M_w/M_n = 1.04$) referred to as PS₁₁₅–PAA₁₅, PS₂₁–PAA₁₅₇, and PS₆₃–PMAA₂₅₁ hereafter, were used in this study. They were purchased from Polymer Source Inc. (Canada) and used as received. As shown in Scheme 1, the azobenzene amphiphile Azo-AOT has a structure based on sodium bis(2-ethylhexyl)sulfosuccinate (AOT), which is the most studied surfactant for reverse micelles. Azo-AOT was designed by inserting two azobenzene moieties between the ionic head and the two bulky alkyl groups of AOT, and its synthetic details will be reported elsewhere.¹⁶ Poly(diallyldimethylammonium chloride) (PDAA; M_w 400000) was obtained from Aldrich and used without further purification. *N,N*-dimethylformamide (DMF), tetrahydrofuran (THF), and *n*-hexane were all analytical-grade products from Beijing Chemical Reagent Co. Quartz slides were purchased from the Changchun Institute of Optics, Fine Mechanics and Physics, Chinese Academy of Sciences.

Preparation of the Azo-AOT-Incorporated Micelle Solution. The block copolymer and Azo-AOT were codissolved in DMF, and after 5 vol % (relative to DMF) deionized water was added, the solution was stirred at 60 °C for 72 h. Then deionized water was slowly added to 20% DMF, and the solution was allowed to dialyze against deionized water for 72 h. The amount of Azo-AOT incorporated into the micelles was estimated by comparing the UV absorbance of the micellar solution at λ_{\max} with those of a series of concentration-known solutions in THF. In this work, micelle 1 denotes the PS₁₁₅–PAA₁₅ micelle incorporating 5 wt % Azo-AOT (saturated), micelle 2 denotes the PS₂₁–PAA₁₅₇ micelle incorporating 10 wt % Azo-AOT, and micelle 3 denotes the PS₂₁–PAA₁₅₇ micelle incorporating 40 wt % Azo-AOT (saturated).

LbL Deposition. The LbL film was assembled on a quartz slide, which was first cleaned by treatment in a hot piranha solution (mixture of 98% H₂SO₄ and 30% H₂O₂ (v/v = 7/3)) for 40 min (caution:

piranha solution is extremely corrosive) and then thoroughly washed with pure water. A hydroxy-tailored quartz slide was then immersed into PDAA aqueous solution. In this way, the substrate was covered with a PDAA layer. After being rinsed with pure water and dried under a nitrogen stream, the resulting substrate was transferred into a solution of Azo-AOT-incorporated PS-*b*-PAA micelles, adding a micelle layer. The immersion time was 10 min in each step. By repeating the above two steps in a cyclic fashion, the LbL multilayer film was fabricated. Both the block copolymer micelles and PDAA were of the same concentration of 1 mg/mL in aqueous solution.

Instruments. UV–vis spectra were obtained on a Hitachi U-3010 spectrophotometer. The irradiation light source for photoisomerization was a high-pressure mercury lamp with an optical fiber (RW-UVA \times 05-100, purchased from Shenzhen Runwing Mechanical & Electrical Co., Ltd., China), and the intensity was 900 mW/cm². The two band-pass filters were of wavelengths 365 ± 10 and 450 ± 10 nm. The irradiation was carried out in an “in situ” mode by irradiating the quartz-supported LbL films or the solutions in the UV–vis spectrophotometer with the optical fiber to minimize the errors in the experiments. Transmission electron microscopy (TEM) was performed on a Hitachi H-800 electron microscope operating at an acceleration voltage of 100 kV. To prepare TEM samples, a drop of the dilute aqueous solution was deposited onto a copper grid, which had been precoated with a thin film of poly(vinyl formal) and then coated with carbon. Two minutes after the deposition, the excess aqueous solution was blotted away with a strip of filter paper. All the samples were stained with 2% phosphotungstic acid hydrate before observation via TEM.

Results and Discussion

Azo-AOT is a molecule with a hydrophilic head and two hydrophobic tails whose structure is quite different from that of normal azobenzene and is suitable to form reverse micelles in a hydrophobic medium (Scheme 1). What happens if a surfactant such as Azo-AOT is incorporated into the block copolymer micelles? To answer this question, we chose PS₁₁₅–PAA₁₅ since it can form a micelle with a relatively larger hydrophobic core and a thinner hydrophilic shell, which is also named a “crew-cut” micelle.¹⁷ When we prepared the Azo-AOT-incorporated micelles at room temperature as usual, it was found that Azo-AOT molecules could not be incorporated into the block copolymer micelles, which might be related to the low compatibility between the two components. Since the micellization of the block copolymer is quite sensitive to the external stimuli, we attempted to raise the temperature of micellization to 60 °C, at which the PS chain of the block copolymer exhibited a higher fluidity than that at room temperature, and successfully incorporated Azo-AOT into PS₁₁₅–PAA₁₅ micelles. The final concentration (saturated) of Azo-AOT is ca. 0.05 mg/mL in 1 mg/mL PS₁₁₅–PAA₁₅ micelle solution. For comparison, PS₂₁–PAA₁₅₇ micelles were used to incorporate Azo-AOT under the same conditions. The UV–vis spectra of the three Azo-AOT-incorporated micelles at the same concentration are shown in Figure 1. Two observations can be made. First, the amount of Azo-AOT incorporated into PS₂₁–PAA₁₅₇ micelles was much larger than that of PS₁₁₅–PAA₁₅ micelles. Second, the wavelengths of the UV absorption peak (λ_{\max}) of Azo-AOT in the three micelles were different, 338 nm in micelle 1 (Figure 1a) and 353 nm in micelle 2 (Figure 1b). Moreover, when the amount of Azo-AOT incorporated into the micelles reached its maximum (micelle 3), λ_{\max} changed to 341 nm, which is similar to that of micelle 1, indicating different aggregating states of azobenzene groups in different micelles. It should be noted that λ_{\max} of Azo-AOT blue-shifted by 15 nm in micelle 1 compared with that in

(15) Wang, Y. P.; Xu, H. P.; Ma, N.; Wang, Z. Q.; Zhang, X.; Liu, J. Q.; Shen, J. C. *Langmuir* **2006**, *22*, 5552.

(16) Wang, G.; Zhao, Y. Manuscript in preparation.

(17) (a) Moffitt, M.; Khogaz, K.; Eisenberg, A. *Acc. Chem. Res.* **1996**, *29*, 95. (b) Chen, D. Y.; Jiang, M. *Acc. Chem. Res.* **2005**, *38*, 494.

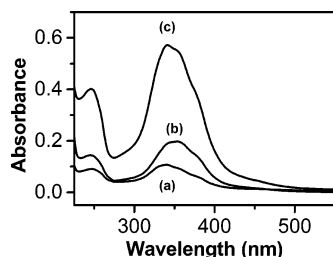


Figure 1. UV-vis spectra of (a) micelle 1 (PS₁₁₅-PAA₁₅ micelle incorporating 5 wt % Azo-AOT (saturated)), (b) micelle 2 (PS₂₁-PAA₁₅₇ micelle incorporating 10 wt % Azo-AOT), and (c) micelle 3 (PS₂₁-PAA₁₅₇ micelle incorporating 40 wt % Azo-AOT (saturated)). The concentration of the block copolymer micelles is kept at 0.04 mg/mL.

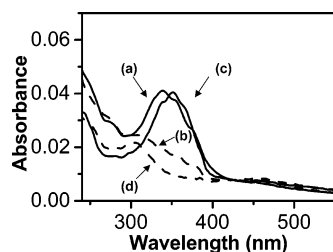


Figure 2. UV-vis spectra of Azo-AOT in different states: (a) *trans*-isomer and (b) *cis*-isomer in reverse micelles in hexane/H₂O, (c) *trans*-isomer and (d) *cis*-isomer in hexane solution. The concentration of Azo-AOT is 0.015 mg/mL.

micelle 2. This blue shift may suggest that Azo-AOT molecules adopt a more compact aggregation state in micelle 2. With the increase of Azo-AOT in the micelles, more and more molecules aggregate in micelle 3, resulting in a blue shift from 353 to 341 nm. There have been some reports in agreement with our results, demonstrating that azobenzene-containing phosphate amphiphiles formed an H-aggregate when the amphiphile self-assembled into a vesicular membrane,¹⁸ which is a more crowded environment for the azobenzene-containing amphiphiles. However, the H-aggregate is rather weak because the UV absorption blue shifts by only 15 nm. To facilitate understanding the aggregating states of Azo-AOT in different block copolymer micelles, the UV spectra of Azo-AOT in the reverse micelles (hexane/H₂O) and diluted solution (hexane) without block copolymers are illustrated in Figure 2. λ_{max} of Azo-AOT in its reverse micelle solution is 338 nm, while it is 351 nm in hexane solution, which is correspondingly similar to λ_{max} of Azo-AOT in micelle 1 and micelle 2. It is shown that, upon UV irradiation, Azo-AOT in the reverse micelles exhibits a UV spectrum similar to that of Azo-AOT in a diluted solution of hexane, which may partially prove that the H-aggregate can be destroyed by UV irradiation to some extent. These results suggest that Azo-AOT molecules adopt an aggregation state similar to that of their reverse micelles in micelle 1 but a solution-like aggregation state in micelle 2. Eisenberg et al. have suggested that when sodium dodecyl sulfate (SDS) is added to the PS-*b*-PAA micelle solution, the hydrocarbon tails of SDS partition into the micellar cores and the SDS itself does not form its bulk micelles.¹⁹ Since Azo-AOT molecules do not prefer to form micellar aggregates in water, we can thus infer that the Azo-AOT molecules may be incorporated into the micellar core in micelle 1 but exist in the boundary between the hydrophobic core and the hydrophilic corona of micelle 2 and micelle 3. Furthermore, it was found that PS₂₁-PAA₁₅₇ micelles

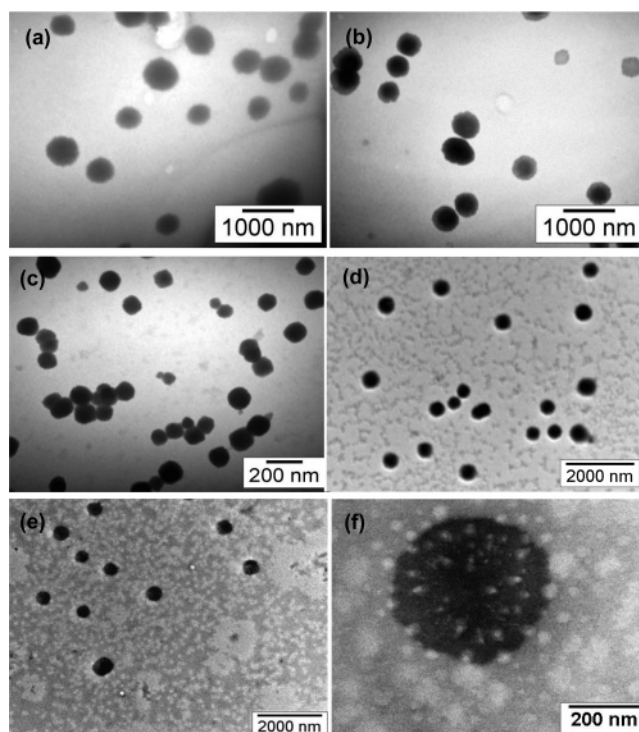


Figure 3. TEM images of (a) empty PS₁₁₅-PAA₁₅ micelles, (b) micelle 1 (PS₁₁₅-PAA₁₅ micelle incorporating 5 wt % Azo-AOT (saturated)), (c) empty PS₂₁-PAA₁₅₇ micelles, (d) micelle 2 (PS₂₁-PAA₁₅₇ micelle incorporating 10 wt % Azo-AOT), (e) micelle 3 (PS₂₁-PAA₁₅₇ micelle incorporating 40 wt % Azo-AOT (saturated)), and (f) a detailed structure of micelle 3.

can incorporate many more Azo-AOT molecules than PS₁₁₅-PAA₁₅ micelles. This phenomenon was quite different from the case when using PS-*b*-PAA micelles to incorporate hydrophobic species,²⁰ in which crew-cut micelles usually have a larger incorporation capacity for hydrophobic dyes than starlike micelles. This result can also agree with the different aggregating states in the three micelles as discussed above. It is found that the length ratio between the hydrophobic PS block and hydrophilic PAA block has a large influence on the aggregating states of Azo-AOT. We have tried to use another block copolymer, poly(styrene-*b*-methacrylic acid) (PS₆₃-PMAA₂₅₁) to coassemble with Azo-AOT. As expected, PS₆₃-PMAA₂₅₁ micelles show incorporating behavior similar to that of PS₂₁-PAA₁₅₇, suggesting that a block copolymer with a relatively shorter PS block may provide Azo-AOT a solution-like environment. As for a block copolymer with a relatively longer PS block, the larger hydrophobic cores may facilitate Azo-AOT to be entirely incorporated into it.

TEM was used to investigate whether there is the morphology change of the micelles before and after incorporation of Azo-AOT. TEM images of "empty" and Azo-AOT-incorporated PS₁₁₅-PAA₁₅ micelles or PS₂₁-PAA₁₅₇ micelles are shown in Figure 3. For PS₁₁₅-PAA₁₅ micelles, the empty ones exhibited spherical aggregates which were quite similar to the Azo-AOT-incorporated ones with sizes of 300–500 nm, suggesting that there were no obvious changes for PS₁₁₅-PAA₁₅ micelles before and after incorporation of Azo-AOT. For PS₂₁-PAA₁₅₇ micelles, the empty ones exhibited a spherical aggregate of about 100 nm and the Azo-AOT-incorporated micelle 2 was enlarged in size to 400–

(18) (a) Whitten, D. G.; Chen, L.; Geiger, H. C.; Perlstein, J.; Song, X. *J. Phys. Chem. B* **1998**, *102*, 10098. (b) Kinoshita, T. *J. Photochem. Photobiol., B* **1998**, *42*, 12. (c) Kuiper, J. M.; Engberts, J. B. F. N. *Langmuir* **2004**, *20*, 1152.

(19) Burke, S. E.; Eisenberg, A. *Langmuir* **2001**, *17*, 8341.

(20) (a) Ma, Y. H.; Cao, T.; Webber, S. E. *Macromolecules* **1998**, *31*, 1773. (b) Teng, Y.; Morrison, M. E.; Munk, P.; Webber, S. E.; Procházka, K. *Macromolecules* **1998**, *31*, 3578. (c) Wang, G. C.; Henselwood, F.; Liu, G. J. *Langmuir* **1998**, *14*, 1554.

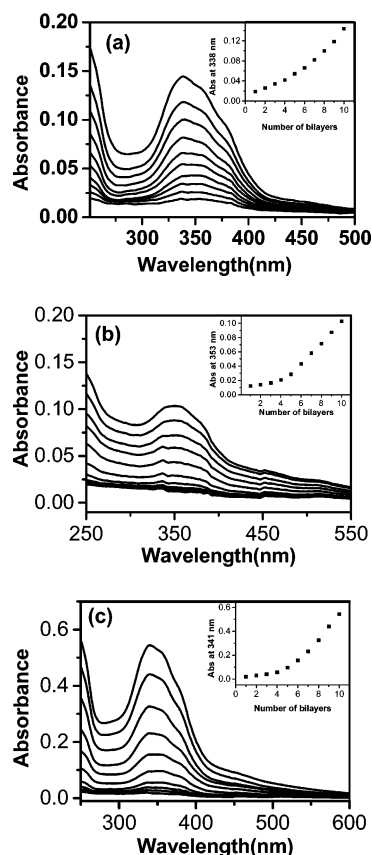


Figure 4. UV–vis spectra of (a) a 10-bilayer PDDA/micelle 1 film, (b) a 10-bilayer PDDA/micelle 2 film, and (c) a 10-bilayer PDDA/micelle 3 film. The insets show the absorbance of Azo-AOT at λ_{\max} in the two films.

500 nm. Interestingly, it is found that, in the TEM image of micelle 3, there are some domains different from the micellar shells, which are probably composed of Azo-AOT. All the sizes of the micelles were larger and the ranges of the micellar sizes were also greater than those of our previous work^{13,15} for the different methods of preparation. Since the micellization of the PS-*b*-PAA block copolymers is greatly influenced by the dynamic factors, it can be rationally inferred that the larger micellar sizes should be related to the higher temperature of micellization than before. Moreover, the micellar structures which we obtained were suitable for incorporation of Azo-AOT molecules.

Since the block copolymer used for micelle formation is poly(styrene-*b*-acrylic acid), it can self-organize into micelles spontaneously with negatively charged shells. Therefore, the Azo-AOT-incorporated polymer micelles can function as negatively charged polymers for alternating deposition with PDDA to form a PDDA/Mic-Azo-AOT multilayer film. The growth of the multilayer film was followed by UV–vis spectra, and the two micelles exhibited different growth behaviors during the LbL fabrication. Figure 4a shows the UV–vis spectra of a 10-bilayer PDDA/micelle 1 multilayer film. The absorption peak at 338 nm can be identified as the π – π^* transition of Azo-AOT in its reverse micelle-like aggregate, which shows that Azo-AOT maintains its aggregation state in the block copolymer micelles during the fabrication of the LbL film. From the insets of Figure 4a we can see that the absorbance at characteristic wavelengths increases in a nonlinear fashion versus the number of deposited bilayers. The nonlinear fashion is very similar to the so-called exponential growth that has been reported else-

Table 1. λ_{\max} of UV–Vis Spectra of Azo-AOT in Different Media^a

medium of Azo-AOT	λ_{\max} (nm)	medium of Azo-AOT	λ_{\max} (nm)
reverse micelles (hexane/H ₂ O) ^b	338	PDDA/micelle 1 LbL film	338
hexane	351	PDDA/micelle 2 LbL film	353
micelle 1	338	PDDA/micelle 3 LbL film	341
micelle 2	353		
micelle 3	341		

^a Micelle 1 = PS₁₁₅–PAA₁₅ micelle incorporating 5 wt % Azo-AOT (saturated), micelle 2 = PS₂₁–PAA₁₅₇ micelle incorporating 10 wt % Azo-AOT, and micelle 3 = PS₂₁–PAA₁₅₇ micelle incorporating 40 wt % Azo-AOT (saturated). ^b The reverse micelles of Azo-AOT were prepared by adding 10 μ L of water to 3 mL of a hexane solution of Azo-AOT under sonication.

Table 2. Photoisomerization Rate Constants of Azo-AOT in Different Media

medium of Azo-AOT	av k_t (s ^{−1})	av k_c (s ^{−1})
micelle 1	1.14×10^{-2}	4.22×10^{-3}
micelle 2	1.89×10^{-2}	6.28×10^{-3}
micelle 3	5.19×10^{-3}	2.25×10^{-3}
PDDA/micelle 1 LbL film	1.25×10^{-2}	6.76×10^{-3}
PDDA/micelle 2 LbL film	1.81×10^{-2}	1.04×10^{-2}
PDDA/micelle 3 LbL film	1.05×10^{-3}	1.25×10^{-3}

where.²¹ For comparison, UV–vis spectra of 10-bilayer PDDA/micelle 2 and PDDA/micelle 3 multilayer films are shown in Figure 4b,c. Similarly, λ_{\max} of Azo-AOT in the (PDDA/micelle 2)₁₀ and (PDDA/micelle 3)₁₀ film is 353 and 341 nm, respectively, being the same as in their micellar solutions. λ_{\max} values of Azo-AOT in different media are summarized in Table 1. λ_{\max} of Azo-AOT was 338 nm for micelle 1 and the PDDA/micelle 1 LbL film and 353 nm for micelle 2 and the PDDA/Micelle 2 LbL film, indicating that Azo-AOT molecules maintained their aggregating states during the fabrication of LbL films.

Photoisomerization of the azobenzene group is a first-order reaction which can be analyzed by the following kinetic equations:¹¹

$$\ln \frac{(A_0 - A_{\text{eq}})}{(A_t - A_{\text{eq}})} = k_t t \quad (1)$$

$$\ln \frac{(A_{\text{eq}} - A_0)}{(A_{\text{eq}} - A_t)} = k_c t \quad (2)$$

where A_0 , A_t , and A_{eq} are the initial absorbance, absorbance at time t , and absorbance at the photostationary state of azobenzene at λ_{\max} , respectively, k_t is the rate constant of *trans*-to-*cis* isomerization, and k_c is the rate constant of *cis*-to-*trans* photoisomerization. Since photoisomerization of azobenzene-containing compounds can be greatly influenced by their aggregating states, we can investigate the photoisomeric behavior of Azo-AOT by analyzing the rate constants of its photoisomerization in different media. The average rate constants of photoisomerization of Azo-AOT in different media are displayed in Table 2. It should be noted that photoisomerization of Azo-AOT in micelle 2 is faster than that in micelle 1 in either *trans*-to-*cis* isomerization or *cis*-to-*trans* isomerization, indicating that the aggregation of Azo-AOT weakened its photoisomerization in PS₁₁₅–PAA₁₅ micelles, while in micelle 3, Azo-AOT molecules undergo the slowest photoisomerization of those in the three

(21) (a) Donald, L.; Elbert, C.; Herbert, B.; Hubbell, J. A. *Langmuir* **1999**, *15*, 5355. (b) Picart, C.; Mutterer, J.; Richert, L.; Luo, Y.; Prestwich, G. D.; Schaaf, P.; Voegel, J.-C.; Lavalle, P. *Proc. Natl. Acad. Sci. U.S.A.* **2002**, *99*, 12531.

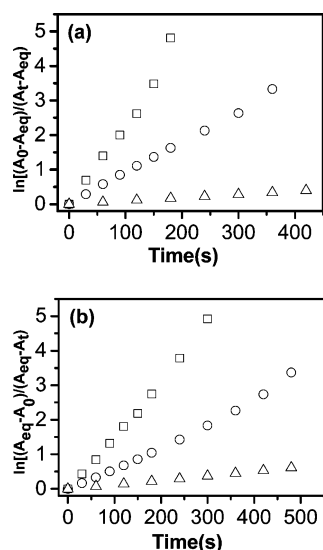


Figure 5. (a) *trans*-to-*cis* photoisomerization and (b) *cis*-to-*trans* photoisomerization of Azo-AOT in a 10-bilayer PDDA/micelle 1 film (circles), a 10-bilayer PDDA/micelle 2 film (squares), and a 10-bilayer PDDA/micelle 3 film (triangles).

micelles, which may be relative to the large incorporation amount of Azo-AOT.

We wondered whether Azo-AOT incorporated into the block copolymer micelles could maintain its photoisomerization properties after deposition onto the PDDA/micelle LbL films. To address this question, a series of irradiation measurements were carried out to investigate the photochromic behavior of Azo-AOT in the PDDA/micelle multilayer films. Plots of *trans*-to-*cis* and *cis*-to-*trans* photoisomerization of Azo-AOT in the two 10-bilayer PDDA/micelle LbL films are shown in Figure 5. We found that Azo-AOT molecules underwent a faster photoisomerization in the PDDA/micelle 2 LbL film than in the PDDA/micelle 1 LbL film and the photoisomerization of Azo-AOT in PDDA/micelle 3 was still the slowest, which was quite similar to the rules of Azo-AOT photoisomerization in the micellar

solutions. The average rate constants of photoisomerization of Azo-AOT in the micelle solutions and PDDA/micelle multilayer films are summarized in Table 2. For the photoisomerization of Azo-AOT, the rate constants in the PDDA/micelle 1 and PDDA/micelle 2 LbL films were very close to those in the micelle solutions, while for the PDDA/micelle 3 multilayer film, the rate constants in the films were smaller than those in the micelle solutions for the photoisomerizations. From this phenomenon we know that, once the micelles incorporate excessive Azo-AOT, the photoresponsibility of the polyelectrolyte/micelle multilayer films will decrease a lot due to the decrease of the free volume in the micelles.

Conclusions

In summary, we used block copolymer micelles as matrixes to incorporate the azobenzene-containing amphiphile Azo-AOT and fabricated the Azo-AOT-incorporated micelles into multilayer films with a polyelectrolyte. This method allowed us to assemble some functional amphiphiles into LbL films, which cannot be assembled by the usual LbL method. It was found, interestingly, that the amount and aggregation states of Azo-AOT in the micelles can be tuned by coassembly with different block copolymers. Thus, Azo-AOT exhibited different photoisomeric rates in different micelles, which is related to the different aggregating states of Azo-AOT in the three micelles. By analyzing the data of UV-vis spectra, we can infer that, in the PS₁₁₅-PAA₁₅ micelles, Azo-AOT adopts an aggregation state similar to that in its reverse micelle but may disperse in the interface between the core and corona of PS₂₁-PAA₁₅₇ micelles. These polyelectrolyte/micelle films incorporating functional amphiphiles have great potential in the field of functional thin films.

Acknowledgment. This work was funded by the National Natural Science Foundation of China (Grants 20334010, 20473045, 50573042, and 20574040) and the National Basic Research Program of China (Grant 2007CB808000). Partial support from the State Key Lab of Polymer Physics and Chemistry is acknowledged too.

LA0632068